Phase Formation and Magnetic Properties of Nb and Fe Co-Doped TiO_2 Nanoparticles Prepared in Ar/O_2 Radio Frequency Induction Thermal Plasma

C.-N. Zhang[1,2], T. Ishigaki[1,3,*], M. Ikeda[1,4], M. Isobe[5], J.-G. Li[1], Y. Moriyoshi[4], H. Hamanaka[4], T. Uchikoshi[1], T. Watanabe[2]

[1] *Nano Ceramic Center, National Institute for Materials Science, Tsukuba, Ibaraki 305-0044, Japan*

[2] *Department of Environmental Chemistry and Engineering, Tokyo Institute of Technology, Yokohama, Kanagawa, 226-8502, Japan*

[3] *Department of Chemical Science and Technology, Hosei University, Koganei, Tokyo 184-8584, Japan*

[4] *Department of Materials Chemistry, Hosei University, Koganei, Tokyo 184-8584, Japan*

[5] *Superconducting Materials Center, National Institute for Materials Science, Tsukuba, Ibaraki 305-0044, Japan*

Abstract: The Nb/Fe co-doped TiO_2 nanopowders have been synthesized via Ar/O_2 RF thermal plasma oxidation, with rutile and anatas phases. In the $Ti_{0.94-y}Nb_{0.06}Fe_yO_2$ nanopowders, weak ferromagnetic at room temperature can be recognized at y=0.001 as the evidenced contribution from doping Nb, whereas the ferromagnetism converts to paramagnetism with increasing the Fe addition content.

Keywords: Nb/Fe co-doped TiO_2, thermal plasma, phase formation, magnetic properties

1. Introduction

Because of TiO_2 exhibiting interesting properties, we have demonstrated the synthesis of pure TiO_2 nanopowders via one-step Ar/O_2 RF thermal plasma oxidizing mists of titanium organometallic compound [1], their phase structure and particle size control via quench-gas injections [2], and the synthesis of doped TiO_2 nanocrystals for photocatalytic [3], magnetic [4], and photoluminescent applications [5-7]. Since the room temperature ferromagnetism (RTF) was reported on Co doped TiO_2 [8], increased attentions have been given to dilute magnetic semiconductors (DMS), due to their potential applications in optoelectronics, magneto-electronics, spintronics, and microwave devices. Very recently, Li et al. [9] have demonstrated that Co^{2+}-doped TiO_2 nanopowders, which were synthesized via one-step Ar/O_2 RF thermal plasma oxidization mists of liquid precursors containing titanium (IV) and cobalt (II) ions, exhibit RTF as an intrinsic nature. In addition, Fe as a magnetic element has similar electronic configuration to Co, resulting in that the study on the magnetic properties of Fe-doped TiO_2 might find helpfulness in understanding the origin of RTF. RTF has been reported with Nb/Fe co-doped TiO_2 thin films [10]. The Nb^{5+} substitution in TiO_2 lattice gives the injection of electronic carrier, and the electronic mediation takes an important role in the RTF properties.

It is noticed that, in majority of the previous studies, Co or Fe-doped TiO_2 was synthesized under vacuum or in reducing atmospheres, giving rise to speculations that in such cases the observed RTF arises from metallic Co or Fe clusters. In contrast to the previous works, we have

synthesized Nb/Fe co-doped TiO_2 nanopowders via Ar/O_2 RF thermal plasma oxidation of atomized liquid precursors containing titanium (IV) butoxide, niobium (V) butoxide and ferrocene (II) in this work. Such an oxidative atmosphere with expectation is to prevent the possibility that formation of any metal elements, and RF thermal plasma can synthesize nanopowders with high crystallinity and homogeneous dopant distribution. All mentioned above were evidenced by analysis in detail given herein. The plasma-generated nanopowders were found to have weak RTF, and detailed characterizations such as XRD, FE-SEM, XPS and magnetic measurements were performed. In the following sections, we report the synthesis process, phase formation and magnetic properties of Nb and Fe co-doped TiO_2 nanoparticles synthesized via RF thermal plasma.

2. Experimental

For powder synthesis, the liquid precursors with the various concentration of dopants (Nb and Fe) in the $Ti_{1-x-y}Nb_xFe_yO_2$ (nominal x=0, 0.02, and 0.06, and y=0, 0.001, 0.005, 0.010 and 0.020) were delivered into the center of the plasma plume through an atomization probe at 3.6 ml/min. Details of precursor preparation and experimental setup and fundamental conditions may be found elsewhere [4].

Phase identification was performed via X-ray diffraction (XRD) on a X-ray diffractometer (RINT 2200, Rigaku, Tokyo, Japan) using nickel-filtered Cu Kα radiation at 40 kV/40 mA operation, with a scanning speed of 0.5°/2θ per minute. Phase composition of the resultant powders were calculated according to the literature [5]. Paricle morphology was observed using a field-emission scanning electron microscope (FE-SEM. Model S-5000, Hitachi, Tokyo, Japan). X-ray photoelectron spectroscopy (XPS) was conducted with monochromatized Al-Kα irradiation (1486.6 eV) at an incident power of 200 W (XPS5700, PHI, Chanhassen, MN, USA); Magnetic properties of the samples were measured on a MPMS-XL commercial instrument (Quantum Design, San Diego, CA, USA).

3. Results and Discussion

3.1 Phase formation

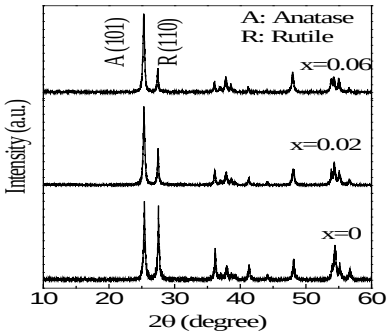

Fig. 1 XRD patterns of the $Ti_{0.98-x}Nb_xFe_{0.02}O_2$ nanopowders. The addition content (x) of Nb is indicated in the figure.

The prescribed addition content of dopants in the liquid precursors have almost been kept to the final products after thermal plasma oxidation, as confirmed by elemental analysis by the inductively couple plasma (ICP) method. Figure 1 exhibits XRD patterns of the $Ti_{0.98-x}Nb_xFe_{0.02}O_2$ nanopowders as the typical resultant products. The doped TiO_2 nanoparticles with the estimated average particle size of 30-50 nm have high crystallinity owing to extremely high synthesis temperature, and consist of stable rutile (JCPDS: No 78-2485) and metastable anatas (JCPDS: No 84-1286) phases. Doping Nb can decreases the rutile weight fraction, as evidenced by the dramatically declined intensity of rutile diffraction peaks (110). It cannot be found that metallic Nb, metallic Fe and other impurity phases are in the XRD patterns, even at higher Nb addition content (x=0.06), indicating that, on one hand, the oxidative atmosphere in the RF thermal plasma indeed ensures the prevention from the formation of any metal elements, on the other hand, Nb has a relatively large solubility in the TiO_2 host lattice, attributed to the

very close ionic radius of Nb^{5+} (0.069 nm) and Ti^{4+} (0.0605 nm).

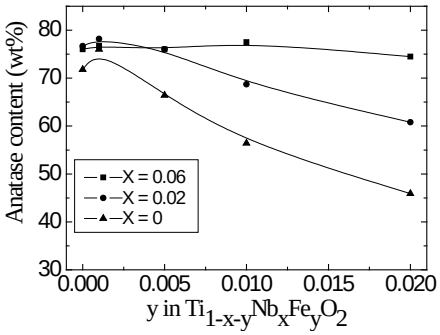

Fig. 2 Phase composition of anatase content in the $Ti_{1-x-y}Nb_xFe_yO_2$ nanopowders.

Figure 2 shows anatase content in the $Ti_{1-x-y}Nb_xFe_yO_2$ nanopowders, as the function of doping Nb and Fe. The anatase content decreases with raising the Fe doping content, but this tendency becomes tardive at a Nb content of x=0.06. This can be understandable from that the incorporation of Fe into TiO_2 host lattice without any Nb can readily create some amount of oxygen vacancies for charge compensation due to different chemical valence, but introducing Nb can play a role for balancing such charge discrepancy in the $Ti_{1-x-y}Nb_xFe_yO_2$ nanopowders, providing the charge compensation to inhibit the formation of oxygen vacancies. In such case, anatase content can be significantly promoted, since the rutile has the greater capability to accept oxygen vacancies than anatase phase, as reported in our previous work [4].

Intensive FE-SEM observation indicates that doping Nb and Fe have not altered the morphology of the plasma-generated powders, which have faceted nanoparticles and nearly spherical submicroparicles, with size ranging from several nanometers up to approximate 100 nm (taking non-doped TiO_2 as example in Fig. 3). Such a wide size distribution and distinctly different particle morphologies might be explained from the various cooling rates of the TiO_2 melt droplets arising from the temperature profile of the thermal plasma and the complex trajectories of the precursor mists [2].

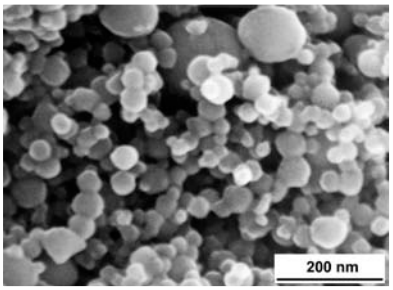

Fig. 3 TEM micrographs showing overall morphology of the non-doped TiO_2 nanoparticles.

The oxidation state of titanium, niobium and iron in the $Ti_{1-x-y}Nb_xFe_yO_2$ was determined through binding energy of $Ti2p_{3/2}$, $Nb3d_{5/2}$ and $Fe2p_{3/2}$ via high-resolution XPS, with various x and y, as shown in Fig. 4. The binding energy are referenced to the O-1s core level of TiO_2 (530.5 eV) to compensate for any possible electrostatic shift caused by charging of the samples during the measurement. The appearance of $Ti2p_{3/2}$ and $Nb3d_{5/2}$ peaks corresponding to ~ 458.4 eV and ~207.3 eV suggest the oxidation state of +4 and +5 for titanium and niobium, respectively. Although it is difficult to unambiguously identify the oxidation state of iron on account of the quite noisy peaks for $Fe2p_{3/2}$, Fe may exist in the $Ti_{1-x-y}Nb_xFe_yO_2$ as oxidation state of +3, due to the oxidative atmosphere in the thermal plasma synthesis process, as stated in our previous work [4]. In addition, it is noteworthy that no any metallic $Nb3d_{5/2}$ peak corresponding to ~202.4 eV can be found in the high-resolution XPS spectrum, thus providing additional evidence that such oxidative atmosphere can also effectively prohibit the formation of Fe. Both cases have been confirmed by XRD (Fig. 1).

3.2 Magnetic properties

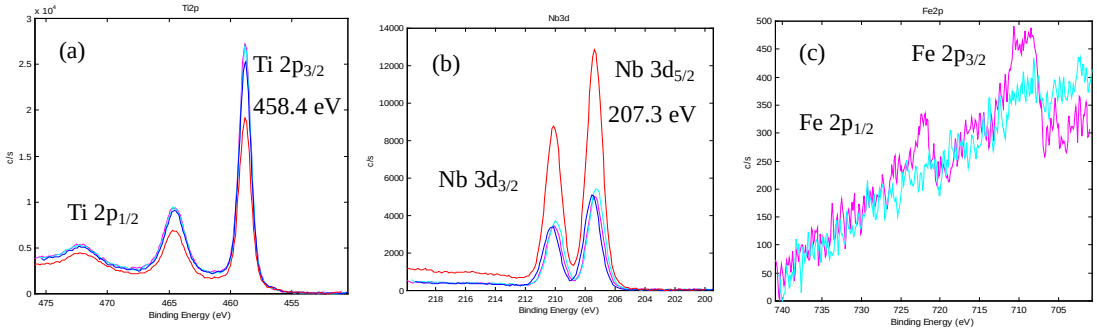

Fig. 4 High-resolution XPS spectra for (a) Ti2p, (b) Nb3d and (c) Fe2p

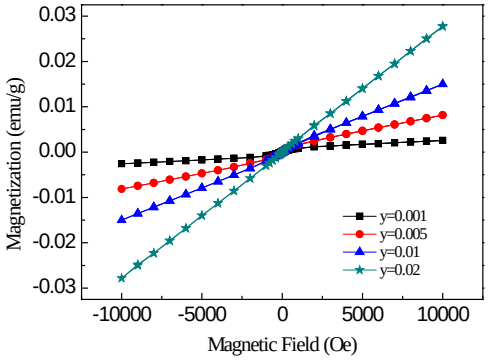

Fig. 5 Magnetization curves of the $Ti_{0.94-y}Nb_{0.06}Fe_yO_2$ nanopowders measured at 300 K. The addition content (y) is denoted in the figure.

Figure 5 presents the magnetic properties of the $Ti_{0.94-y}Nb_{0.06}Fe_yO_2$ nanopowders at 300 K. The existence of hysteresis can be recognized at y=0.001 as shown in Fig. 5, indicative of weak ferromagnetic at room temperature as the evidenced contribution from doping Nb, as the Fe-doped TiO_2 nanopowders synthesized in RF thermal plasma are paramagnetic in nature at room temperature in our previous report [4]. Such case can be explained from that doping Nb in the $Ti_{0.94-y}Nb_{0.06}Fe_yO_2$ nanopowders can enhance the carrier concentration and mobility in the sample when y=0.001, and ferromagnetism for DMS materials is very sensitive to carrier as a carrier-mediated exchange [10]. Nevertheless, it can be seen in Fig. 5 that the ferromagnetism converts to paramagnetism with increasing the Fe addition content, ascribed to that the increase of rutile arising from the oxygen vacancies at higher Fe addition content, and the carriers in rutile are known have much lower mobility (1-2 orders of magnitude) than those in anatase [10].

References

[1] J.-G. Li, H. Kamiyama, X.H. Wang, Y. Moriyoshi, T. Ishigaki, J. Euro. Ceram. Soc., **26**, 423 (2006).

[2] J.-G. Li, M. Ikeda, R. Ye, Y. Moriyoshi, T. Ishigaki, J. Phys. D: Appl. Phys., **40**, 2384 (2007).

[3] X. H. Wang, J.-G. Li, H. Kamiyama, Y. Moriyoshi, T. Ishigaki, J. Phys. Chem. B, **110**, 6804 (2006).

[4] X. H. Wang, J.-G. Li, H. Kamiyama, M. Katada, N. Ohashi, Y. Moriyoshi, T. Ishigaki, J. Am. Chem. Soc., **127**, 10982 (2005).

[5] J.-G. Li, X. H. Wang, K. Watanabe, T. Ishigaki, J. Phys. Chem. B, **110**, 1121 (2006).

[6] J.-G. Li, X. H. Wang, C. C. Tang, T. Ishigaki, S. Tanaka, J. Am. Ceram. Soc., **91**, 2032 (2008).

[7] T. Tachikawa, T. Ishigaki, J.-G. Li, M. Fujitsuka, T. Majima, Angew. Chem. Int. Ed., 47, 5348 (2008).

[8] Y. Matsumoto, M. Murakami, T. Shono, T. Hasegawa, T. Fukumura, M. Kawasaki, P. Ahmet, T. Chikyow, S. Koshihara, H. Koinuma, Science, 291, 854 (2001)

[9] J.-G. Li, R. Büchel, M. Isobe, T. Mori, T. Ishigaki, J. Phys. Chem. C (in press).

[10] T. Hitotsugi, Y. Furubayashi, K. Inaba, Y. Hirose, K. Nakajima, T. Chikyow, T. Shimada, T. Hasegawa, J. Appl. Phys., 99, 08M121 (2006).